

Regulating Charge Diffusion of Two-Dimensional Cobalt-Iron Hydroxide/Graphene Composites for High-Rate Water Oxidation

Tang Tang,^{ab} Wen-Jie Jiang,^a Lu-Pan Yuan,^{ab} Shuai Niu,^{ab} Jin-Song Hu,^{ab} and Li-Jun Wan**^{ab}

a. Beijing National Laboratory for Molecular Sciences (BNLMS), CAS Key Laboratory of Molecular Nanostructure and Nanotechnology, Institute of Chemistry, Chinese Academy of Sciences (CAS), Beijing 100190, China;

E-mail: hujs@iccas.ac.cn, wanlijun@iccas.ac.cn

b. University of Chinese Academy of Sciences, Beijing 100049, China.

This file includes Fig. S1-S17 and Table S1-S3

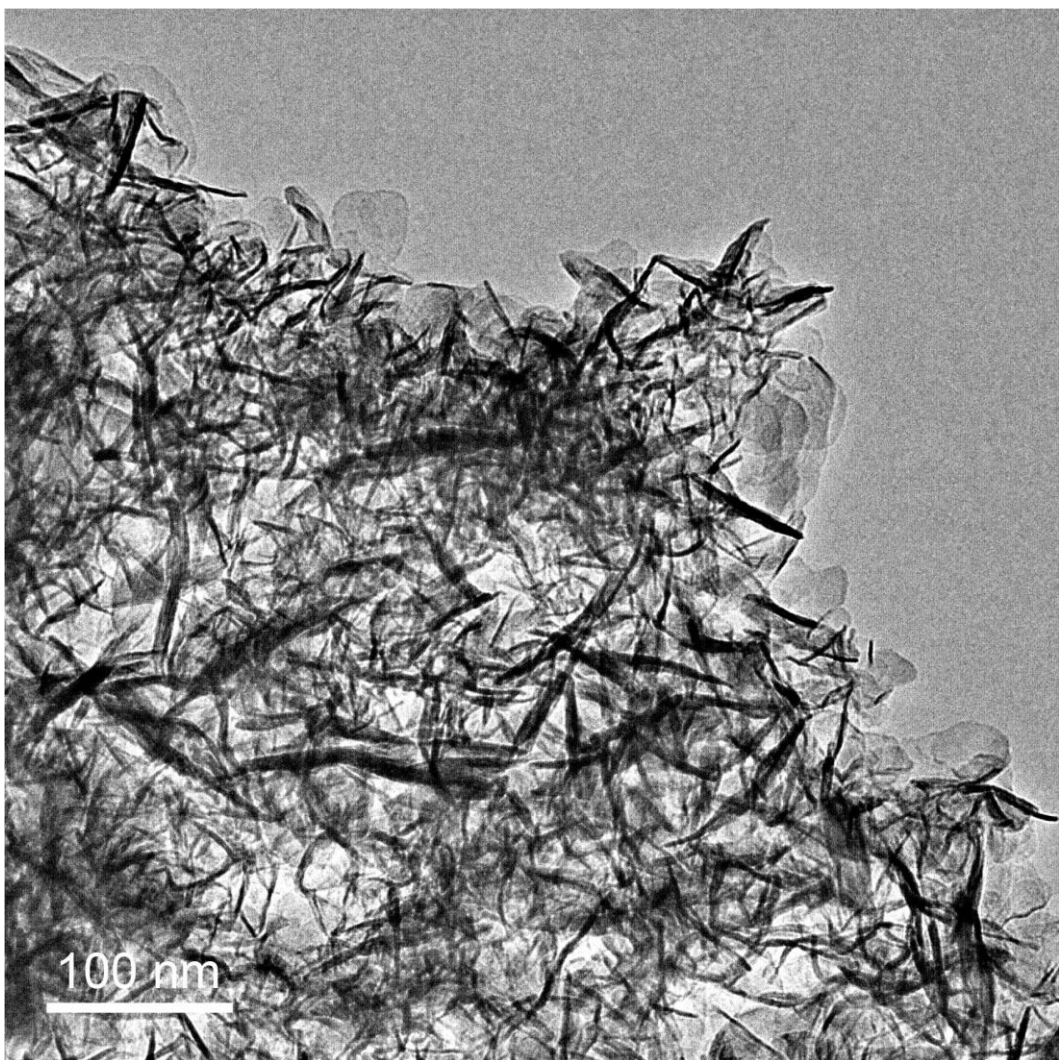


Fig. S1 TEM image of CFH@G-3.75

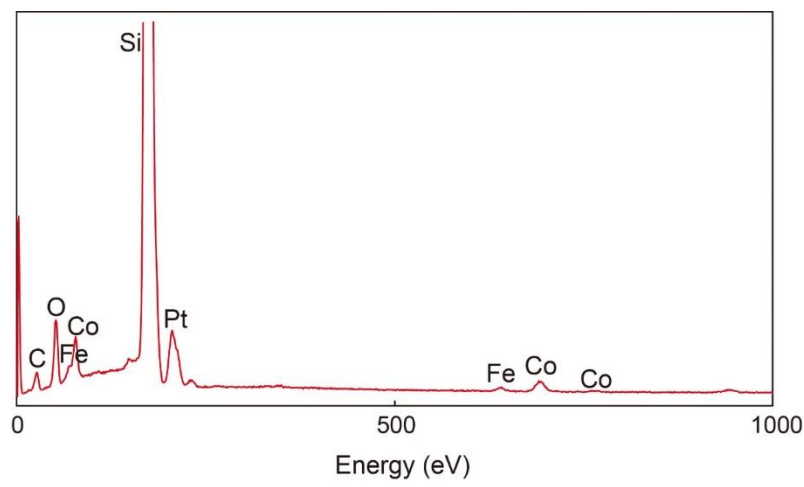


Fig. S2 EDS spectrum of CFH@G-1.5. Pt signal comes from the sputtered Pt layer for SEM observation.

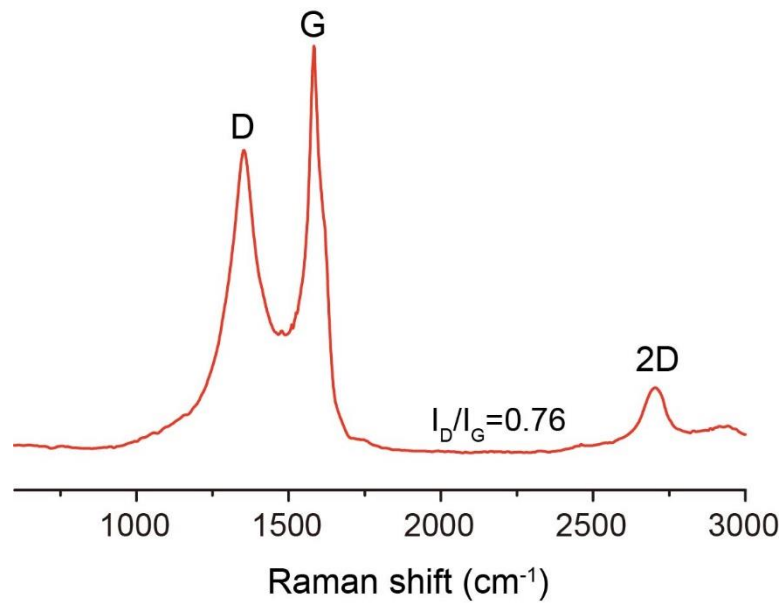


Fig. S3 Raman spectrum of the graphene substrate.

The Raman spectrum of the chemical method prepared graphene substrate shows a strong D-band peak, indicating the graphene surface containing abundant defects.

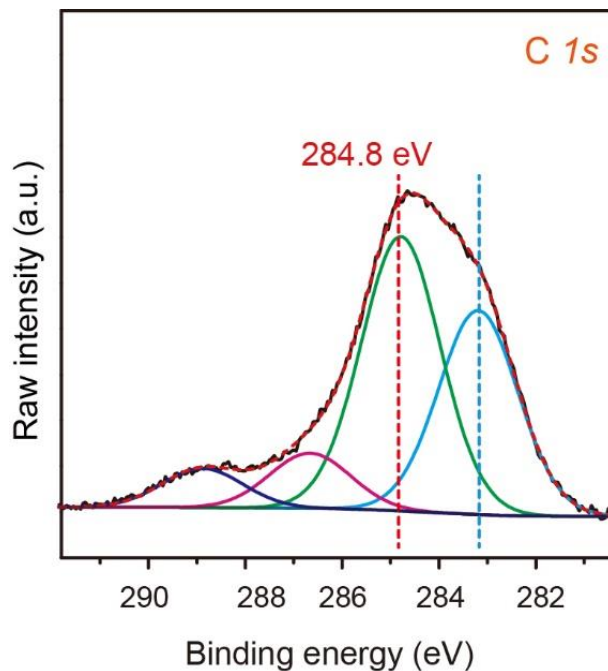


Fig. S4 XPS spectrum of C 1s for CFH@G-0.375.

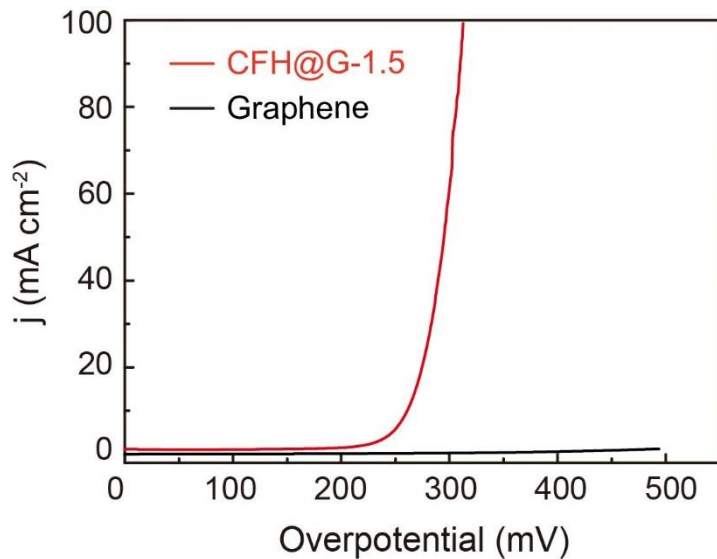


Fig. S5 Steady OER polarization curves of CFH@G-1.5 and graphene substrate.

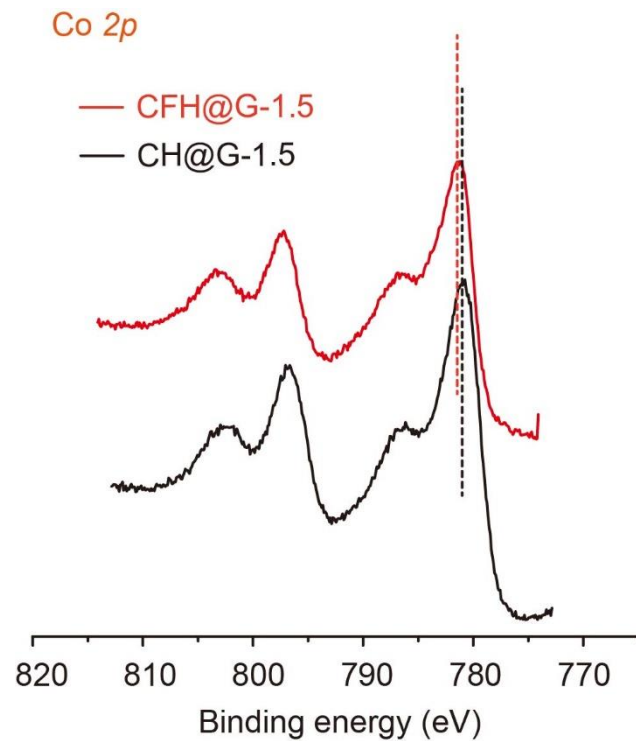


Fig. S6 Co 2p spectra of Co hydroxide/graphene (CH@G-1.5) and CFH@G-1.5.

After introducing Fe, the Co $2p_{3/2}$ binding energy is shifted from 781.1 eV of pure CH@G-1.5 to 781.3 eV (CFH@G-1.5), indicating the modulation of Co active site by Fe.

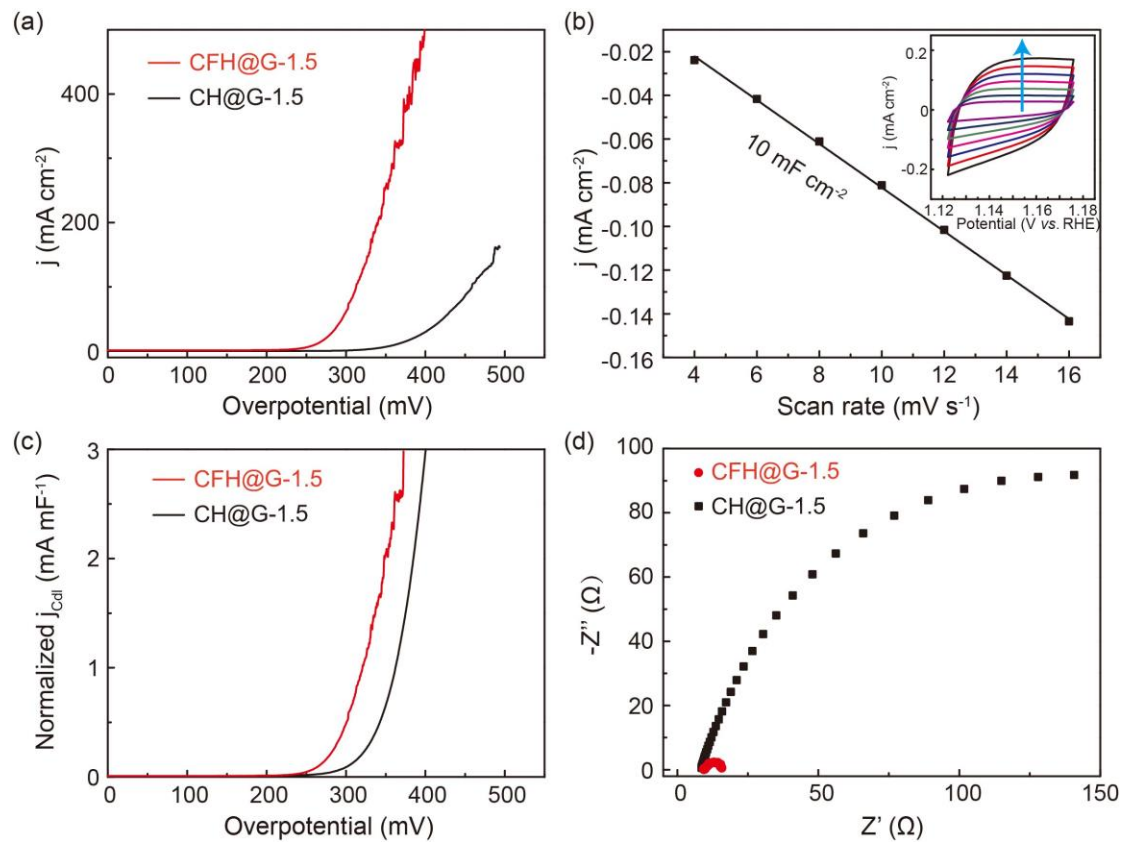


Fig. S7 (a) OER polarization curves, (b) the relationship plots between current density and different scan rates (4, 6, 8, 10, 12, 14, and 16 mV s^{-1} as displayed inset), (c) OER polarization curves normalized by C_{dl} , and (d) EIS Nyquist plots at 1.53 V (vs. RHE) for CH@G-1.5 and CFH@G-1.5.

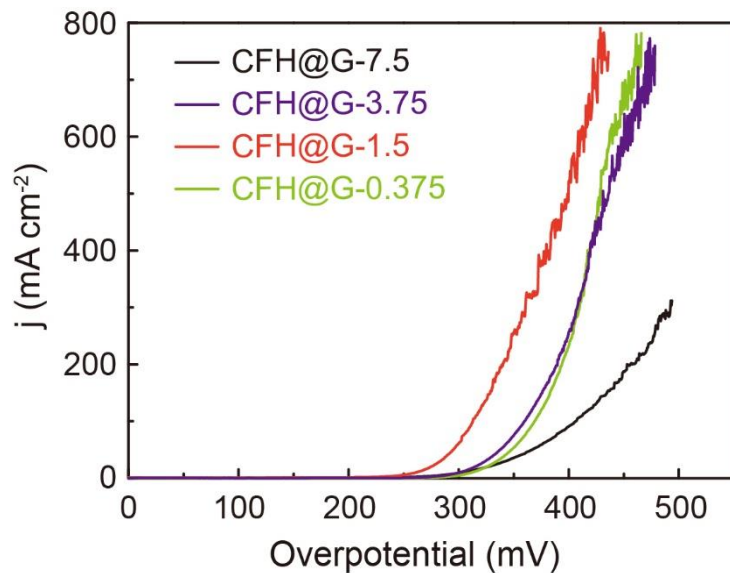


Fig. S8 OER polarization curves of four CFH@G catalysts at large current density scale.

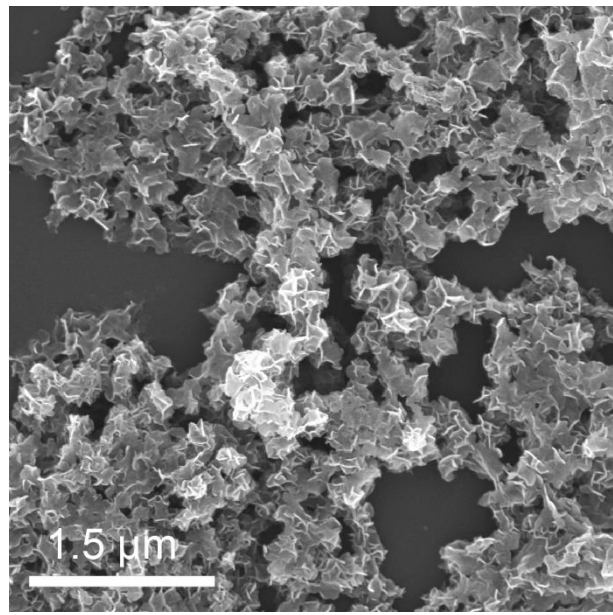


Fig. S9 SEM image of CFH-1.5 prepared without the addition of graphene.

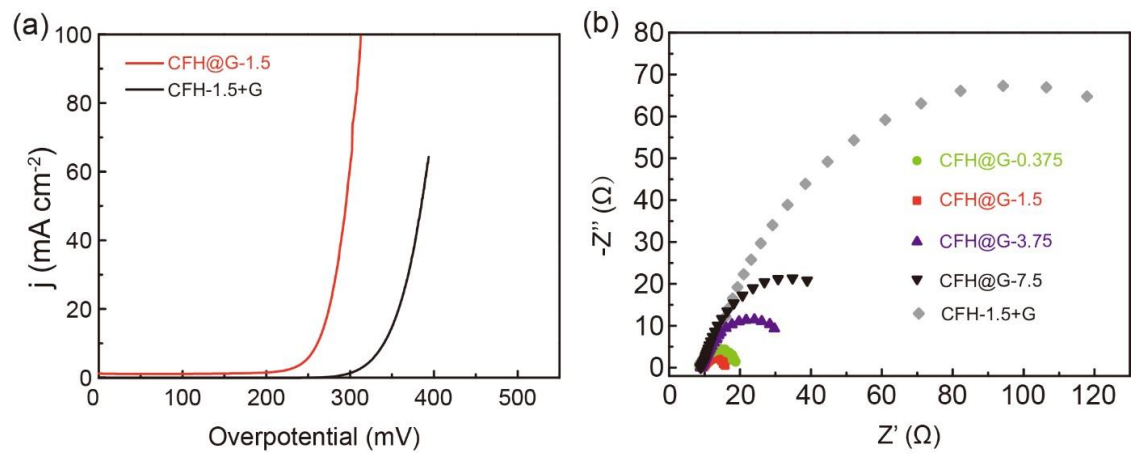


Fig. S10 (a) OER polarization curves of CFH@G-1.5 and CFH-1.5+G. (b) EIS Nyquist plots at 1.53 V (*vs.* RHE) of four CFH@G catalysts and CFH-1.5+G.

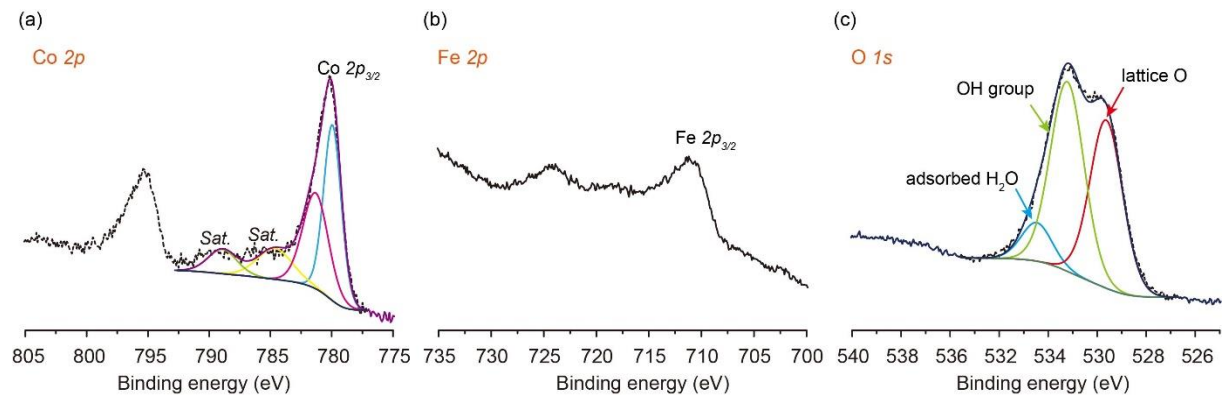


Fig. S11 XPS spectra of (a) Co 2p, (b) Fe 2p, and (c) O 1s for CFH@G-1.5 after long time durability test.

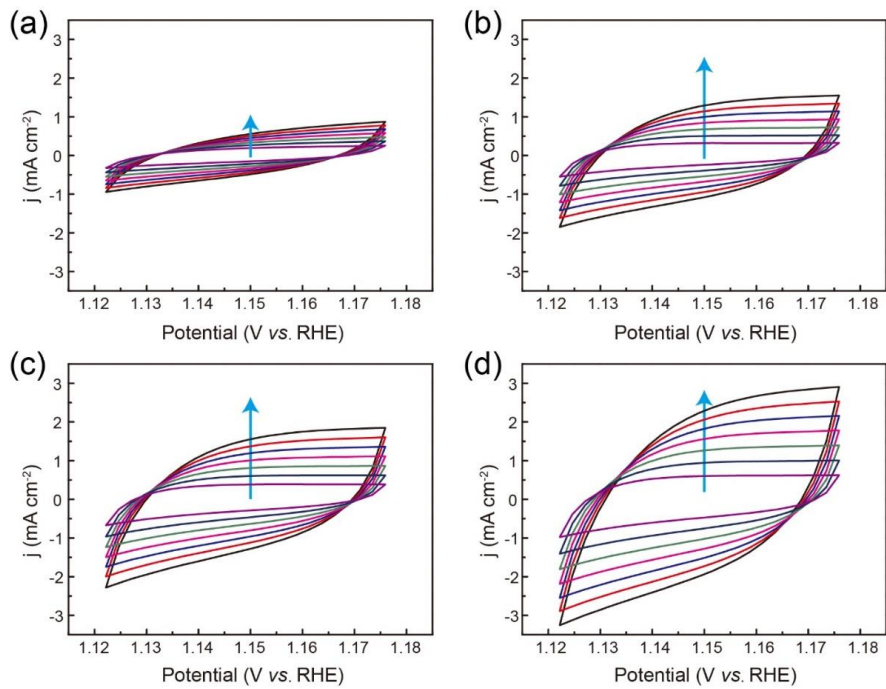


Fig. S12 Cyclic voltammograms at various scan rates of 4, 6, 8, 10, 12, 14, and 16 mV s^{-1} for (a) CFH@G-0.375, (b) CFH@G-1.5, (c) CFH@G-3.75, and (d) CFH@G-7.5.

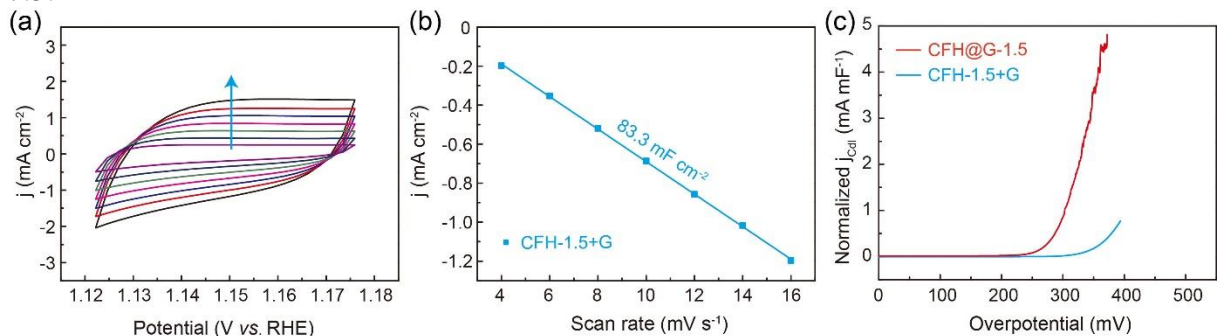


Fig. S13 (a) Cyclic voltammograms at various scan rates of 4, 6, 8, 10, 12, 14, and 16 mV s^{-1} and (b) the relationship plots between current density and scan rates of CFH-1.5+G. (c) OER polarization curves normalized by C_{dl} for CFH@G-1.5 and CFH-1.5+G.

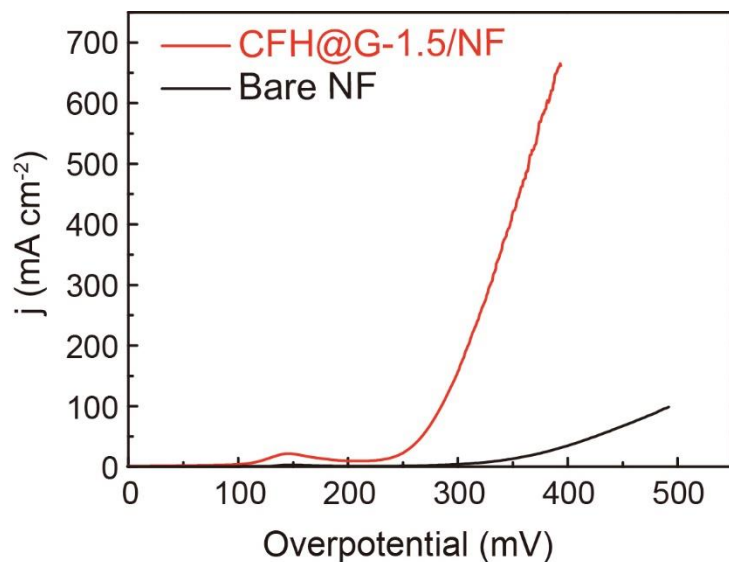


Fig. S14 OER polarization curves of CFH@G-1.5/NF and bare NF substrate.

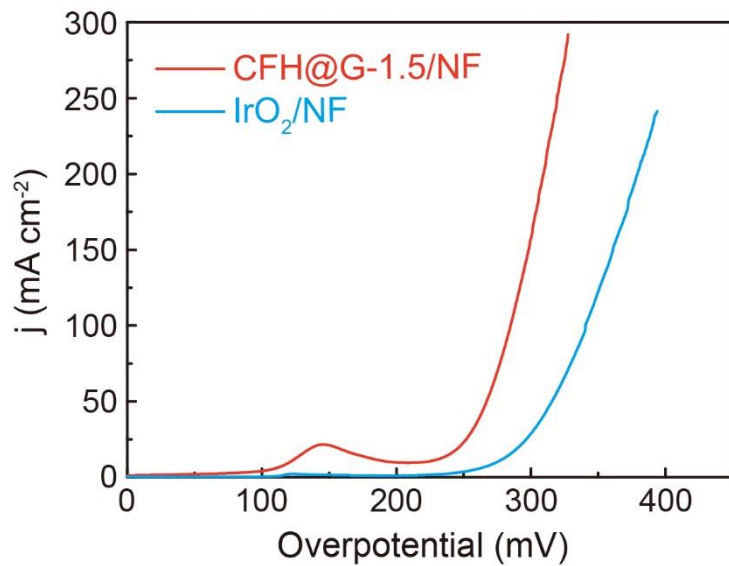


Fig. S15 OER polarization curves of CFH@G-1.5/NF and IrO₂/NF.

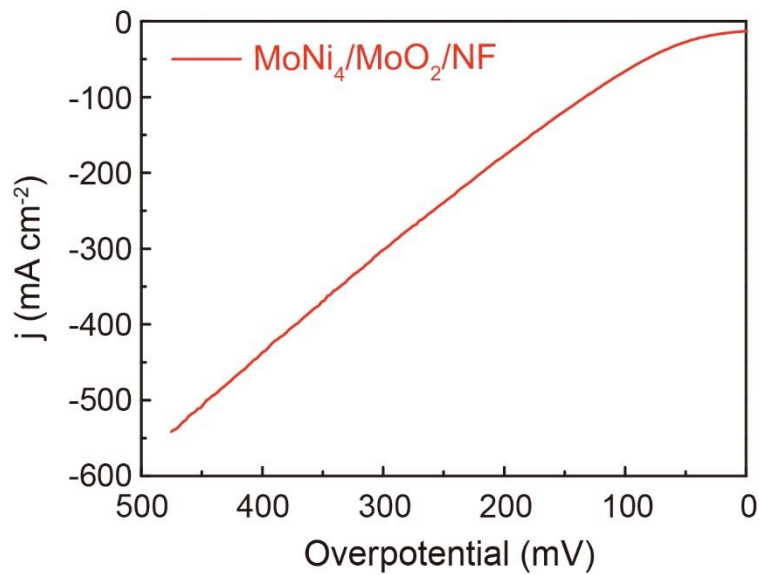


Fig. S16 HER polarization curve of $\text{MoNi}_4/\text{MoO}_2/\text{NF}$ without iR-compensation.

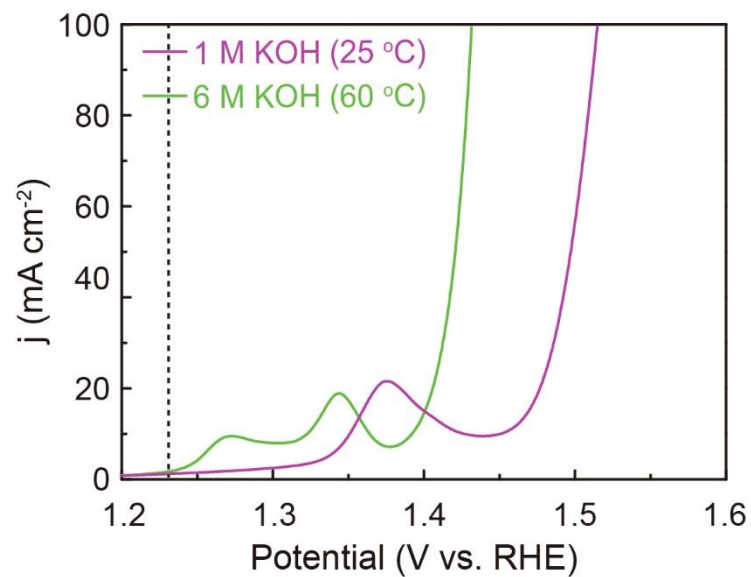


Fig. S17 OER polarization curves of CFH@G-1.5/NF at 1 M KOH (25 °C) and 6 M KOH (60 °C)

Table S1 Comparison of OER catalytic performance of various state-of-the-art electrocatalysts in 1 M KOH.

Catalysts	Overpotential (mV) at current density of			Reference
	10 mA cm ⁻²	100 mA cm ⁻²	500 mA cm ⁻²	
CFH@G-1.5	260	312	398	
CFH@G-1.5/NF	246@20	284	364	This work
CFH@G-1.5/NF (6 M KOH@60 °C)	176@20	200	231 277@2000	
Co phosphide/phosphate	300	-	-	Adv. Mater., 2015, 27, 3175.
Co-P/NC	319	~420	-	Chem. Mater., 2015, 27, 7636.
Co ₁ Mn ₁ CH/NF	294@30	349	~410	J. Am. Chem. Soc., 2017, 139, 8320.
NiCo ₂ S ₄ /NF	-	470	-	Adv. Funct. Mater., 2016, 26, 4661.
FeNiOOH(Se)/IF	222	279	348	J. Am. Chem. Soc., 2019, 141, 7005
NiFeRu-LDH	225	260	-	Adv. Mater., 2018, 30, 1706279.
Fe-CoOOH/G	330	405	-	Adv. Energy Mater., 2017, 7, 1602148.
NiCo@NiCoO ₂ /C PMRAs	366@20	~420	-	Adv. Mater., 2018, 30, 1705442.
(Ln _{0.5} Ba _{0.5})CoO _{3-δ}	~350	-	-	Nat. Commun., 2013, 4, 2439.
PrBa _{0.5} Sr _{0.5} Co _{1.5} Fe _{0.5} O _{5+δ}	~358	-	-	Nat. Commun., 2017, 8, 14586.
Fe–CoP/Ti	230	310	-	Adv. Mater., 2017, 29, 1602441.
NF@NC–CoFe ₂ O ₄ /C NRAs	240	300	-	Adv. Mater., 2017, 29, 1604437.
pc-Ni-B _i @NB	302	-	-	Angew. Chem. Int. Ed., 2017, 56, 6572.
N-Ni ₃ S ₂ /NF 3D	-	330	-	Adv. Mater., 2017, 29, 1701584.
NiFe LDH- NS@DG10	210	-	-	Adv. Mater., 2017, 29, 1700017.
S,N-Fe/N/C-CNT	370	-	-	Angew. Chem. Int. Ed., 2017, 56, 610.
CuNiN/FeNiCu	300	400	-	Nat. Commun., 2018, 9, 2326.
CoO/CoFeO	297	370	-	Adv. Mater., 2018, 30, 1801211.
NiCo/NiCoO	332	430	-	Adv. Mater., 2018, 30, 1705442.
Co/Ni ₃ N	307	-	-	Adv. Mater., 2018, 30, 1705516.
NiFeSe cages	240	270	-	Adv. Mater., 2017, 29, 1703870.

Table S2 Comparison of overall water splitting performance of various state-of-the-art electrocatalysts in 1 M KOH.

Catalysts	Potential (V) at current density of		Reference
	10 mA cm ⁻²	100 mA cm ⁻²	
CFH@G-1.5/NF // MoNi₄/MoO₂/NF	1.507@20	1.696	
CFH@G-1.5/NF // MoNi₄/MoO₂/NF (6 M KOH@60 °C)	1.439@20	1.556 1.694@400	This Work
EG/Co _{0.85} Se // NiFe-LDH	1.67	-	Energy Environ. Sci., 2016, 9, 478.
NiFe LDH/NF	1.7	-	Science, 2014, 345, 1593.
Ni ₅ P ₄	1.7	~2.1	Angew. Chem. Int. Ed., 2015, 54, 12361.
NiCoP/rGO	1.59	-	Adv. Funct. Mater., 2016, 26, 6785.
Co-CoO _x /CN	1.6	>2.0	J. Am. Chem. Soc., 2015, 137, 2688.
Co-P/NC	1.71	~1.95	Chem. Mater., 2015, 27, 7636.
NiCo ₂ O ₄ /NF	1.84	>2.0	Adv. Funct. Mater., 2016, 26, 4661.
Co ₁ Mn ₁ CH/NF	1.68	~1.98	J. Am. Chem. Soc., 2017, 139, 8320.
NiCo ₂ O ₄	1.65	-	Angew. Chem. Int. Ed., 2016, 55, 6290.
NiFe/Ni(OH) ₂ /NiAl // NiMo/Ni(OH) ₂ /NiAl	1.59	-	Adv. Sci., 2017, 4, 1700084.
Ni ₂ P/NF	1.63	-	Energy Environ. Sci., 2015, 8, 2347.
FeNiOOH(Se)/IF // MoNi ₄ /MoO ₂ /NF	1.55@20	~1.71	J. Am. Chem. Soc., 2019, 141, 7005
NiFeV-LDHs	1.591	~1.82	Small, 2018, 14, 1703257.
NiFe-NiMo	1.51	-	Nat. Commun., 2018, 9, 2014.
NiFeO _x /CFP	1.51	~1.78	Nat. Commun., 2015, 6, 7261.
Fe–CoP	1.60	-	Adv. Mater., 2017, 729, 602441.
NiFe LDH-NS@DG	1.50@20	-	Adv. Mater., 2017, 29, 1700017.
Se-(NiCo)S/OH	1.60	~2.08	Adv. Mater., 2018, 30, 1705538.
CoP/NCNHP	1.64	~1.95	J. Am. Chem. Soc., 2018, 140, 2610.
Co ₃ O ₄ microtube arrays	1.63	~1.98	Angew. Chem. Int. Ed., 2017, 56, 1324.
Ni-Co-P hollow nan bricks	1.62	~1.98	Energy Environ. Sci., 2018, 11, 872.
np-Co _{1.04} Fe _{0.96} P	1.53	~1.61	Energy Environ. Sci., 2016, 9, 2257.

Table S3 Comparison of overall solar-to-hydrogen conversion efficiency in recent reports and this work.

Electrochemical cell	Solar cell	STH efficiency	Electrolyte	Reference
CFH@G-1.5/NF // MoNi ₄ /MoO ₂ /NF	GaAs	17.41%	1 M KOH	This work
FeNiOOH(Se)/IF // MoNi ₄ /MoO ₂ /NF	GaAs	18.55%	1 M KOH	J. Am. Chem. Soc., 2019, 141, 7005.
MHCM // NiMoS	GaInP/GaAs/Ge 3jn	17.9%	Sea water	Adv. Mater., 2018, 30, 1707261.
NiFe LDH // CrNN	GaAs	15.1%	1 M KOH	Angew. Chem. Int. Ed., 2015, 54, 11989.
MEA electrolyzer, IrO _x // Pt	c-Si 3p	14.2%	Water, pH 7	J. Electrochem. Soc., 2016, 163, 1177.
NiFe LDH // NiP	Lead halide (CH ₃ NH ₃ PbI ₃) perovskite 2p	12.7%	pH 13.6/BPM/pH 0.9	Adv. Energy. Mater., 2016, 6, 1600100.
NiFe LDH // NiFe LDH	Lead halide (CH ₃ NH ₃ PbI ₃) perovskite 2p	12.3%	1 M NaOH	Science, 2014, 345, 1593.
Na:NiFeO _x // NiP	Lead halide (CH ₃ NH ₃ PbI ₃) perovskite 2p	11.22%	1 M KOH	Energy Environ. Sci., 2017, 10, 121.
Pt // Pt	CuInGaSe ₂ 3p	10.5%	3 M H ₂ SO ₄	Energy Environ. Sci., 2013, 6, 3676.
Ni-Bi // NiMoZn	c-Si 4p	10.0%	0.5 M KBi	Proc. Natl. Acad. Sci. U. S. A., 2014, 111, 14057.
CoMnO@CN	Silicon	8%	1 M KOH	J. Am. Chem. Soc., 2015, 137, 14305.
Ni // Pt	PBDTTPD:PCBM/PEDOT:PSS 3jn	6.1%	1 M NaOH	Adv. Mater., 2016, 28, 3366.
Co-Bi // NiMoZn	a-Si 3jn (wired device)	4.7%	0.5 M KBi	Science, 2011, 334, 645.
CuCoO-NW	Silicon	4.5%	1 M KOH	Adv. Funct. Mater., 2016, 26, 8555.